Theory of Optical Parametric Oscillation Internal to the Laser Cavity

M. KENNETH OSHMAN, MEMBER, IEEE, AND STEPHEN E. HARRIS, MEMBER, IEEE

Abstract—Since the fields inside a laser cavity are much higher than the external fields, an analysis of a parametric oscillator with the nonlinear crystal internal to the laser is performed. Using self-consistency equations as the starting point, the equations of motion of such an oscillator are derived. Depending on various cavity, pumping, and nonlinearity parameters, these lead to several types of oscillation with distinctly different operating characteristics: (1) efficient parametric oscillation similar to that of previous analyses; (2) inefficient parametric oscillation resulting from the fact that the nonlinear interaction drives the phases rather than the amplitudes of the signal, idler, and pump; and (3) a pulsing output from the oscillator with repetitive pulses of the signal and idler. A stability analysis of these various regions shows that they are mutually exclusive and can be experimentally chosen by changing the laser gain, the oscillator output coupling, or the strength of the nonlinear interaction. It is shown that the internal oscillator efficiency rapidly approaches the Manley–Rowe limit, as the available pump power becomes several times greater than that required for threshold. The efficiency of an external oscillator having a triply resonant optical cavity is found to be generally less than that of the corresponding internal oscillator.

I. Introduction

IN THIS PAPER we examine the theory of optical frequency parametric oscillation with the nonlinear crystal placed inside the cavity of the pumping laser. Such an oscillator, proposed originally by Kroll [1], takes advantage of the high pump fields inside the laser cavity, compared to outside, in overcoming threshold and in leading to efficient conversion of pump power to signal and idler power. Several authors have discussed the enhancement of second harmonic generation under similar conditions [2], [3].

With the theory of optical parametric oscillation well known at lower frequencies [4], the extensions to optical frequencies have been considered by a number of authors [1], [5]–[12]. Much of the theoretical apparatus necessary for understanding optical frequency parametric oscillation has been developed to handle the specific problem of harmonic generation although extension to the case of parametric oscillation is straightforward. This includes calculations of the effects of phase matching [7], [13]–[17], focusing [5], [18], [19], double refraction [7], [17], [20], [21], and optical frequency resonators [22], [23]. A number of experiments have been performed involving parametric amplification [8], [24]–[27], and in 1965, Giordmaine and Miller [28] reported the first observation of tunable parametric oscillation. Since that time, several other observations of pulsed parametric oscillation have been reported [29]–[31] and recently Smith *et al.* [32] have observed CW parametric oscillation.

Fig. 1 is a schematic representation of a possible internal parametric oscillator with the pump, signal, and idler simultaneously resonated. In this noncollinear configuration, the interaction region is reduced; however, the problems of multiple wavelength antireflection coatings and mirror coatings characteristic of a collinear configuration are avoided. Two-dimensional parametric amplification of this sort has been observed external to the laser by Akhmanov *et al.* [26]. For analytical simplicity we consider the case of collinear interactions, although the extension to the noncollinear case is straightforward. Such an oscillator might be achieved experimentally using a dichroic beam splitter to divert the signal and idler while allowing the pump to travel through the laser medium.

The analysis leads to the surprising result that an internal parametric oscillator can operate in several previously unpredicted regimes. Briefly, there are three regions of operation: 1) an efficient regime with operating characteristics similar to those of previous analyses; 2) an inefficient regime in which the parametric coupling drives the phases rather than the amplitudes of the oscillations and wherein an interesting shift of signal, idler, and pump frequencies from their normal positions is observed; and 3) a repetitively pulsing regime characterized by short pulses of output power at the signal and idler, accompanied by nearly simultaneous decreases in power at the pump. These results are due basically to the fact that the signal and idler are coupled directly to the saturating gain mechanism of the pumping laser through the nonlinear interaction. The choice of parameters necessary for operation in a particular regime is discussed in terms of the stability conditions for the various types of operation.

After considering the internal oscillator, one is led to question the fundamental difference between it and an oscillator consisting of cavities external to the laser, which again resonate signal, idler, and pump. Again for high-Q cavities, the pump fields could be very high. Experimentally, the differences are immediately apparent. The difficulties of placing the crystal inside the laser cavity

Manuscript received March 29, 1968; revised May 10, 1968. The work reported in this paper was sponsored by the National Aeronautics and Space Adminstration under NASA Grant NGR-05-020-103. M. K. Oshman's work was partially supported by Sylvania Electronic Systems through the Independent Research Program. Portions of this paper were presented at the 1966 Conference on Electron Device Research.

M. K. Oshman was with the Department of Electrical Engineering, Stanford University. He is now with Sylvania Electronic Systems, Mountain View, Calif.

S. E. Harris is with the Department of Electrical Engineering, Stanford University, Stanford, Calif.

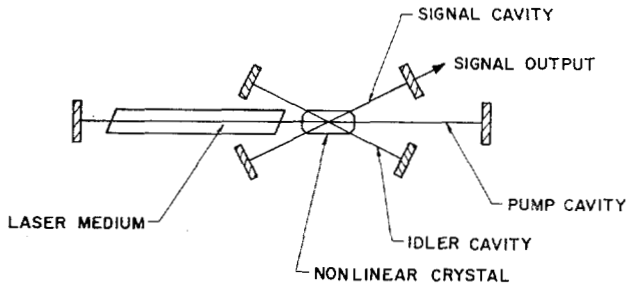

Fig. 1. One geometical arrangement of an internal parametric oscillator.

are large; however, based on other work that uses crystals inside a laser cavity, these seem to be problems that can be overcome. On the other hand, the difficulty of efficiently coupling the pump into an external oscillator is tremendous. Nevertheless, assuming one could optimally couple the pump into such an oscillator, the question remains as to the relative performance of the internal and external oscillator. In particular, as the external oscillator goes above threshold, the pump experiences reflections from the active cavity, thus reducing the efficiency of the oscillator. Similar reflections at microwave frequencies were observed by Ho and Siegman [33]. In Section IV, the efficiency of the external oscillator is compared to that of the internal oscillator, and it is apparent that reflections do render the external oscillator less efficient.

II. Equations of Motion for the Internal Parametric Oscillator

In deriving the equations of motion of the internal parametric oscillator, we use a technique similar to that used by Harris and McDuff [34] to analyze the FM laser. We use the self-consistency equations developed by Lamb [35], which describe the effect of an arbitrary optical polarization on the optical frequency electric fields of a high-Q multi-mode resonator. We direct our attention to three modes of interest with circular frequencies ω_1, ω_2, ω_3 satisfying the relation $\omega_1 + \omega_2 = \omega_3$. In the usual terminology of parametric interactions then ω_1, ω_2, and ω_3 are the signal, idler, and pump frequency, respectively. We shall label all quantities referring to the signal mode, idler, and pump with the subscripts 1, 2, and 3, respectively.

Neglecting transverse variations, the total electric field in the cavity can be written as

$$E(x, t) = \sum_{i=1}^{3} E_i(t) \cos [\omega_i t + \phi_i(t)] u_i(x), \tag{1}$$

where E_i is the amplitude of the ith mode and $u_i(x)$ is the spatial variation of the ith mode, which has circular frequency Ω_i and is that mode lying closest in frequency to ω_i. We normalize u_i such that

$$\int_0^L u_i u_j \, dx = \delta_{ij}, \tag{2}$$

where we have let the cavity extend from $x = 0$ to $x = L$. The self-consistency equations then are

$$[\omega_i + \dot{\phi}_i - \Omega_i] E_i = -\frac{1}{2}\left(\frac{\omega_i}{\epsilon}\right) C_i \tag{3}$$

$$\dot{E}_i + \frac{1}{2}\left(\frac{\omega_i}{Q_i}\right) E_i = -\frac{1}{2}\left(\frac{\omega_i}{\epsilon_0}\right) S_i. \tag{4}$$

Here Q_i is the Q of the ith mode resulting from the losses due to transmission, scattering, absorption, and diffraction. In deriving these equations, Q_i arises through the definition of a ficticious volume conductivity σ_i, which accounts for these losses. The Q_i and σ_i are related by

$$Q_i = \frac{\omega_i \epsilon_0}{\sigma_i}. \tag{5}$$

We will eventually divide σ_i into two parts, one resulting from volume loss effects and the other resulting from transmission through the mirrors. The C_i and S_i are related to the total polarization $P(x, t)$ through the following equations:

$$\begin{aligned} P_i(t) &= \int_0^L P(x, t) u_i(x) \, dx \\ &= C_i(t) \cos [\omega_i t + \phi_i(t)] \\ &\quad + S_i(t) \sin [\omega_i t + \phi_i(t)]. \end{aligned} \tag{6}$$

In writing these self-consistency equations, $E_i(t)$ and $\phi_i(t)$ are assumed slowly varying with respect to ω_i.

In considering parametric interactions inside the laser, the polarization at a particular frequency will have two contributions. One primarily affects the pump and results from the presence of the laser medium. The other results from the nonlinear interactions of the electric fields at other frequencies.

The contribution to the polarization due to the laser medium can be introduced as macroscopic quadrature and in-phase components of susceptibility. Then we have

$$C_i(t) = \epsilon_0 \chi_i' E_i(t) \tag{7a}$$

and

$$S_i(t) = \epsilon_0 \chi_i'' E_i(t). \tag{7b}$$

We assume that the signal and idler frequencies are well removed from any transitions of the laser medium, so contributions to them are essentially negligible. For the pump χ_3'' accounts for gain and saturation due to the laser medium; χ_3' results in frequency shifts and mode pulling and pushing effects.

In proceeding to the calculation of the parametric contribution to the polarization, we shall use the specific example of lithium niobate ($LiNbO_3$) as the nonlinear element [36]. This is useful in performing the analysis; however, the technique can easily be generalized to any parametric system. In particular, with $LiNbO_3$, we can assume phase matching is achieved for propagation at 90° to the optic axis [37], as used in the experiments of Giordmaine and Miller [28]. In this way, we can avoid the problems of double refraction, which would needlessly complicate this analysis.

For $LiNbO_3$ oriented with its crystallographic x-axis

along the x-axis of the cavity, the polarization in the crystal is related to the electric fields by

$$P_y(x, t) = 2d_{15}E_yE_z \tag{8}$$

and

$$P_z(x, t) = d_{31}E_y^2. \tag{9}$$

The subscripts y and z refer to fields polarized along the y- and z-axes of the crystal. We shall assume that the signal and idler are ordinary rays polarized along the y-axis and the pump is an extraordinary ray polarized along the z-axis. We should point out that (8) and (9) relate the time-dependent nonlinear polarization to the time-dependent electric fields. Normally, the value of d is defined by relating the Fourier amplitude of the nonlinear polarization to the Fourier amplitudes of the electric fields. Therefore, as discussed by Pershan [38], *the numerical value of d in these equations is a factor of* 2 *larger than commonly quoted values.*

Using (8) and (9) in conjunction with (1) and (6), we therefore find the following parametric contributions to the polarization (Kleinman's symmetry condition [39] is assumed so that $d_{15} = d_{31}$):

$$C_1(t) = \delta E_2E_3 \cos(\phi_3 - \phi_1 - \phi_2) \tag{10a}$$

$$S_1(t) = -\delta E_2E_3 \sin(\phi_3 - \phi_1 - \phi_2) \tag{10b}$$

$$C_2(t) = \delta E_1E_3 \cos(\phi_3 - \phi_1 - \phi_2) \tag{10c}$$

$$S_2(t) = -\delta E_1E_3 \sin(\phi_3 - \phi_1 - \phi_2) \tag{10d}$$

$$C_3(t) = \delta E_1E_2 \cos(\phi_3 - \phi_1 - \phi_2) \tag{10e}$$

$$S_3(t) = \delta E_1E_2 \sin(\phi_3 - \phi_1 - \phi_2). \tag{10f}$$

Here δ is defined by

$$\delta = d_{15}\int_0^{L'} u_1(x)u_2(x)u_3(x)\,dx, \tag{11}$$

where we have assumed the crystal extends from $x = 0$ to $x = L'$. All contributions at frequencies well removed from the frequencies ω_1, ω_2, and ω_3 are neglected.

In evaluating δ we shall assume that the mirrors of the resonator represent a short-circuit surface for the signal and the idler and an open-circuit surface for the pump. Then the spatial variation of the modes inside the crystal is of the form

$$u_1(x) = \left(\frac{2}{L}\right)^{1/2} \sin k_1x \tag{12a}$$

$$u_2(x) = \left(\frac{2}{L}\right)^{1/2} \sin k_2x \tag{12b}$$

$$u_3(x) = \left(\frac{2}{L}\right)^{1/2} \cos k_3x. \tag{12c}$$

The reason for choosing these boundary conditions is apparent upon inspection of the expression for δ. If all three modes had short-circuit boundaries, then δ would be zero with no parametric interaction. This is the problem met in second harmonic generation where both the fundamental and pump are resonated [40], and results from the fact that a polarization wave is 90° out of phase with the electromagnetic wave it radiates. We define the phase mismatch in terms of the wave vectors as

$$\Delta k = k_3 - k_2 - k_1, \tag{13}$$

and retain only low-frequency terms in (11) with the result

$$\delta = -\left(\frac{2}{L}\right)^{1/2} \frac{L'}{L}\, d_{15}\, \frac{\sin \Delta kL'}{\Delta kL}. \tag{14}$$

In practice phase matching can be achieved at 90° to the optic axis by varying the temperature of the crystal [41], [42].

We now combine (6), (7), and (10) with (3) and (4). Since the dielectric constant in the crystal is substantially different from ϵ_0, when using (10) in (3) and (4), we replace ϵ_0 with ϵ, where ϵ is the dielectric constant of the crystal and is approximately the same at ω_1, ω_2, and ω_3. Then one finds

$$\dot{E}_1 = -A_1E_1 + \frac{\omega_1\delta}{2\epsilon} E_2E_3 \sin(\phi_3 - \phi_1 - \phi_2) \tag{15a}$$

$$\dot{E}_2 = -A_2E_2 + \frac{\omega_2\delta}{2\epsilon} E_1E_3 \sin(\phi_3 - \phi_1 - \phi_2) \tag{15b}$$

$$\dot{E}_3 = -A_3E_3 - \frac{\omega_3\delta}{2\epsilon} E_1E_2 \sin(\phi_3 - \phi_1 - \phi_2) \tag{15c}$$

$$\dot{\phi}_3 - \dot{\phi}_2 - \dot{\phi}_1 = -\Omega' + \frac{\delta}{2\epsilon}\left[\frac{\omega_3E_1E_2}{E_3} - \frac{\omega_1E_2E_3}{E_1} - \frac{\omega_2E_1E_3}{E_2}\right] \cdot \cos(\phi_3 - \phi_1 - \phi_2), \tag{15d}$$

where

$$A_1 = \frac{\omega_1}{2}\left[\frac{1}{Q_1} + \chi_1''\right] \tag{16a}$$

$$A_2 = \frac{\omega_2}{2}\left[\frac{1}{Q_2} + \chi_2''\right] \tag{16b}$$

$$A_3 = \frac{\omega_3}{2}\left[\frac{1}{Q_3} + \chi_3''\right] \tag{16c}$$

$$\Omega' = [\omega_3\chi_3' - \omega_2\chi_2' - \omega_1\chi_1']/2. \tag{17}$$

In treating the gain and saturation of the laser, we need to assume some functional form for χ_3''. There have been several different saturation functions suggested for describing the observed effects of various lasers. In this analysis we use a small-signal approximation similar to that derived by Lamb [35]. With this approximation, χ_3'' is related to the single-pass power gain by

$$\frac{\omega_3L}{c}\chi_3'' = -g_0(1 - \beta E_3^2), \tag{18}$$

where g_0 is the single-pass unsaturated power gain and β is a parameter accounting for the effects of saturation.

A more realistic saturation function for inhomogeneously broadened lasers is represented by [43]

$$\frac{\omega_3L}{c}\chi_3'' = -\frac{g_0}{(1 + 2\beta E_3^2)^{1/2}}. \tag{19}$$

The saturation function of (18) produces essentially the same results as (19) under the condition that

$$\left(\frac{g_0}{\alpha_3}\right)^2 - 1 \ll 1,$$

where α_3 is the single-pass power loss. There are a few low-gain lasers, such as Nd : YAG, under which this condition might well be satisfied. Further, we argue that for internal parametric oscillation, the signal and idler drain much of the laser power, thus not permitting the pump to saturate fully. Nevertheless, the reason for using the saturation function of (18) is its simplicity. We have carried out the entire subsequent analysis using (19) and find the same qualitative results. Since the objective here is to point out the general behavior of internal parametric oscillation, we believe the use of the small-signal saturation function is justified. In any particular application, one would have to calculate the following results, using the appropriate saturation function and appropriate parameters.

If we change the time variable so that $\tau = (c/2L)t$, then (15) and (16) become

$$\frac{dE_1}{d\tau} = -\alpha_1 E_1 + \omega_1 \kappa E_2 E_3 \sin(\phi_3 - \phi_1 - \phi_2) \tag{20a}$$

$$\frac{dE_2}{d\tau} = -\alpha_2 E_2 + \omega_2 \kappa E_1 E_3 \sin(\phi_3 - \phi_1 - \phi_2) \tag{20b}$$

$$\frac{dE_3}{d\tau} = -\alpha_3 E_3 + g_0(1 - \beta E_3^2)E_3 - \omega_3 \kappa E_1 E_2 \sin(\phi_3 - \phi_1 - \phi_2) \tag{20c}$$

$$\frac{d}{d\tau}(\phi_3 - \phi_1 - \phi_2) = \Omega + \kappa\left[\frac{\omega_2 E_1 E_2}{E_3} - \frac{\omega_1\omega_2\omega_3}{E_1} - \frac{\omega_2 E_1 E_3}{E_2}\right] \cdot \cos(\phi_3 - \phi_1 - \phi_2), \tag{20d}$$

where

$$\alpha_1 = \frac{L\omega_1}{c}\left[\frac{1}{Q_1} + \chi_1''\right] \tag{21a}$$

$$\alpha_2 = \frac{L\omega_2}{c}\left[\frac{1}{Q_2} + \chi_2''\right] \tag{21b}$$

$$\alpha_3 = \frac{L\omega_3}{c}\left[\frac{1}{Q_3}\right] \tag{21c}$$

$$\Omega = \frac{L}{c}[\omega_3\chi_3' - \omega_2\chi_2' - \omega_1\chi_1'] \tag{21d}$$

and

$$\kappa = \frac{L\delta}{\epsilon c}. \tag{22}$$

Here α_i is the single-pass power loss for the ith mode. These equations are similar in form to the general equations of motion for parametric interactions described by Siegman [44]. The main difference arises due to the introduction of a saturating gain mechanism. For that reason we believe the form of the subsequent results is generally applicable to other parametric systems coupled directly to the gain mechanism of the pump.

III. Operating Characteristics of the Internal Parametric Oscillator

Using (20a) to (20d) we are in a position to investigate the operating characteristics of the internal parametric oscillator. Previous analyses of parametric oscillators have resulted in the well-known threshold conditions for oscillation and one steady-state region of parametric oscillation. Below threshold, the signal and idler remain zero, whereas above threshold, the pump limits at the threshold level and additional pump power is converted to signal and idler power.

As opposed to this previous solution, the internal parametric oscillator displays three distinct steady-state regions of operation. One region of operation results in the expected behavior, which predicts efficient conversion of pump power to signal power. In addition there is another CW output of the oscillator wherein the phases rather than the amplitudes of the signal and idler are driven by the nonlinear interaction, thereby resulting in less efficient operation. Finally, there is a continuous relaxation oscillation type of solution. In this case the signal and idler spike on and off, resulting in a repetitively pulsing output from the oscillator.

A. Steady-State Solutions for the Internal Parametric Oscillator

Equations (20a) to (20d) produce three distinct steady-state solutions found by setting all derivatives with respect to τ equal to zero. For the following solutions we assume that the mode pulling term Ω is equal to zero. First for the case where there is no parametric interaction ($\kappa = 0$) we have

$$E_1 = E_2 = 0 \tag{23a}$$

$$E_3^2 = \frac{g_0 - \alpha_3}{g_0\beta}. \tag{23b}$$

Equation (23b) predicts the steady-state amplitude of the laser field. For future calculations it is convenient to find the output power of the laser. To do so we divide α_3, the single-pass power loss of the laser, into two parts and let

$$\alpha_3 = \alpha_{3c} + \alpha_{3d}, \tag{24}$$

where α_{3c} is that part of the loss resulting from output coupling and α_{3d} is that part of the loss attributed to all other dissipative mechanisms. Then the output power of the laser P_3 is proportional to $\alpha_{3c}E_3^2$ so

$$P_3 = \gamma\alpha_{3c}E_3^2, \tag{25}$$

where γ is the constant of proportionality. Maximizing P_3 with respect to α_{3c}, the maximum output power of the laser is

$$P_{3,\max} = \gamma\frac{(g_0 - \alpha_{3d})^2}{4g_0\beta}. \tag{26}$$

In the presence of parametric interaction, the first steady-state solution is found by taking $\kappa \neq 0$ and $\phi_3 -$

$\phi_1 - \phi_2 = \pi/2$. Then the cosine term of (15d) is zero, the sine terms of (15a) to (15d) are one, and

$$E_1^2 = \frac{1}{\omega_2\omega_3\kappa^2}\left[(g_0 - \alpha_3)\alpha_2 - g_0\beta\frac{\alpha_1\alpha_2^2}{\omega_1\omega_2\kappa^2}\right] \tag{27a}$$

$$E_2^2 = \frac{1}{\omega_1\omega_3\kappa^2}\left[(g_0 - \alpha_3)\alpha_1 - g_0\beta\frac{\alpha_1^2\alpha_2}{\omega_1\omega_2\kappa^2}\right] \tag{27b}$$

$$E_3^2 = \frac{\alpha_1\alpha_2}{\omega_1\omega_2\kappa^2}. \tag{27c}$$

This is the usual efficient solution for parametric oscillation.

The final steady-state solution is found by assuming $\phi_3 - \phi_1 - \phi_2 =$ a constant $\neq \pi/2$:

$$E_1^2 = \frac{\omega_1}{\omega_3}\frac{\alpha_1 + \alpha_2}{\alpha_1}E_3^2 \tag{28a}$$

$$E_2^2 = \frac{\omega_2}{\omega_3}\frac{\alpha_1 + \alpha_2}{\alpha_2}E_3^2 \tag{28b}$$

$$E_3^2 = \frac{g_0 - \alpha_1 - \alpha_2 - \alpha_3}{g_0\beta} \tag{28c}$$

$$\sin^2(\phi_3 - \phi_1 - \phi_2) = \frac{g_0\beta\alpha_1\alpha_2}{g_0 - \alpha_1 - \alpha_2 - \alpha_3}\frac{1}{\omega_1\omega_2\kappa^2}. \tag{28d}$$

B. Stability Criteria for Steady-State Solutions

Since there are several steady-state solutions for the internal oscillator, we must find the necessary conditions that a particular solution be stable. There are a number of techniques for approaching this problem, including Liapunov's stability criteria [45] and the Hurwitz test [46], both of which were used. We quote only the results. At the outset we should point out that we find the stability conditions of the various regions to be mutually exclusive. That is, two steady-state solutions are not simultaneously possible.

As is expected, the stability of the free running laser solution is guaranteed so long as parametric oscillation is not possible. That is, below a certain level of pump power, the signal and idler are zero. This condition (for stability of the laser with no parametric oscillation) is just the inverse of the threshold condition for parametric oscillation and is given by

$$E_3^2 = \frac{g_0 - \alpha_3}{g_0\beta} < \frac{\alpha_1\alpha_2}{\omega_1\omega_2\kappa^2}. \tag{29}$$

Stability of the first steady-state parametric oscillation solution (27a) to (27c) requires that three conditions be satisfied. First there is the threshold condition:

$$\frac{g_0 - \alpha_3}{g_0\beta} > \frac{\alpha_1\alpha_2}{\omega_1\omega_2\kappa^2}. \tag{30}$$

The second condition requires that if the single-pass gain of the laser is greater than the sum of the loss to the pump, signal, and idler, i.e.,

$$g_0 > \alpha_1 + \alpha_2 + \alpha_3,$$

then for stability,

$$\frac{g_0 - \alpha_1 - \alpha_2 - \alpha_3}{g_0\beta} < \frac{\alpha_1\alpha_2}{\omega_1\omega_2\kappa^2}. \tag{31}$$

This second condition proves to be the condition that the steady-state solution of (28a) to (28d) not be stable. Finally, there is a third stability condition given by the rather complicated relation

$$\frac{g_0 - \alpha_3}{g_0\beta} < \frac{\alpha_1\alpha_2}{2\omega_1\omega_2\kappa^2}\left[1 + 5\sqrt{1 + \frac{24\alpha_1\alpha_2(\alpha_1 - \alpha_2)^2}{\{(\alpha_1 + \alpha_2)(\alpha_1 + \alpha_2 + \alpha_3 - g_0) - 10\alpha_1\alpha_2\}^2}}\right] + \frac{(\alpha_1 + \alpha_2)(\alpha_1 + \alpha_2 + \alpha_3 - g_0)}{4}\left[1 - \sqrt{1 + \frac{24\alpha_1\alpha_2(\alpha_1 - \alpha_2)^2}{\{(\alpha_1 + \alpha_2)(\alpha_1 + \alpha_2 + \alpha_3 - g_0) - 10\alpha_1\alpha_2\}^2}}\right]. \tag{32}$$

For a better feeling of what this relation entails we assume that the signal loss equals the idler loss, i.e., $\alpha_1 = \alpha_2$, in which case (32) becomes

$$\frac{g_0 - \alpha_3}{g_0\beta} < \frac{3\alpha_1\alpha_2}{\omega_1\omega_2\kappa^2}.$$

This shows that the free running laser power should be less than three times that required for parametric threshold.

This last stability requirement is connected with the third type of operation of the oscillator previously described—the pulsing output. If this condition (32) is not satisfied, then the output of the oscillator consists of a continuous train of pulses. The solution for this region cannot be solved in closed form; however, we have performed a detailed computer solution of this region, which is described in Section III-E.

Finally, for the second steady-state parametric oscillation solution (28a) to (28d) to be stable, it is necessary that

$$g_0 > \alpha_1 + \alpha_2 + \alpha_3 \tag{33}$$

and

$$\frac{g_0 - \alpha_1 - \alpha_2 - \alpha_3}{g_0\beta} > \frac{\alpha_1\alpha_2}{\omega_1\omega_2\kappa^2}. \tag{34}$$

C. Efficient Internal Parametric Oscillation

In describing the characteristics of the various regions of operation of the internal parametric oscillator, it is convenient to define a parameter κ_{th}. This parameter represents that value of κ necessary to overcome threshold in the absence of any output coupling loss to the pump, signal, or idler and is given therefore by the relation

$$\kappa_{th}^2 = \frac{\alpha_{1d}\alpha_{2d}}{\omega_1\omega_2}\frac{g_0\beta}{g_0 - \alpha_{3d}}, \tag{35}$$

where we have divided α_i into two components such that

$$\alpha_i = \alpha_{ic} + \alpha_{id}. \tag{36}$$

Experimentally, κ is variable by adjusting phase-matching

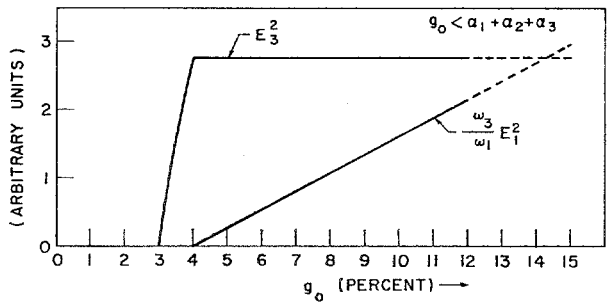

Fig. 2. Pump and signal power inside resonator versus single-pass laser gain in region of efficient parametric oscillation.

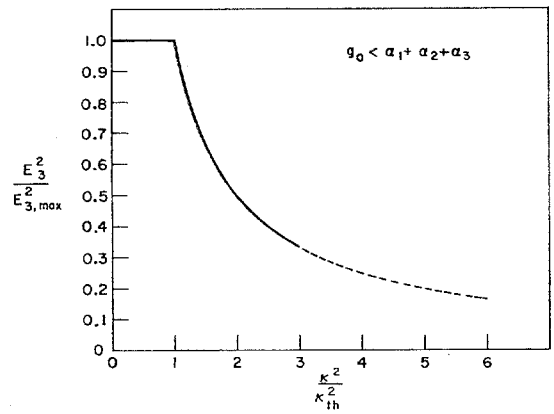

Fig. 3. Pump power inside resonator versus $(\kappa/\kappa_{th})^2$ in region of efficient parametric oscillation.

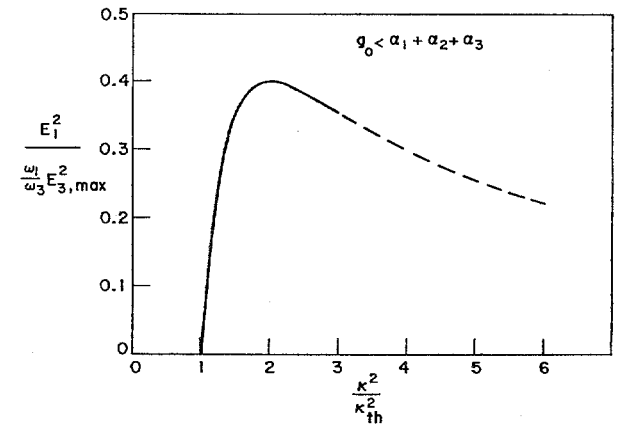

Fig. 4. Signal power inside resonator versus $(\kappa/\kappa_{th})^2$ in region of efficient parametric oscillation.

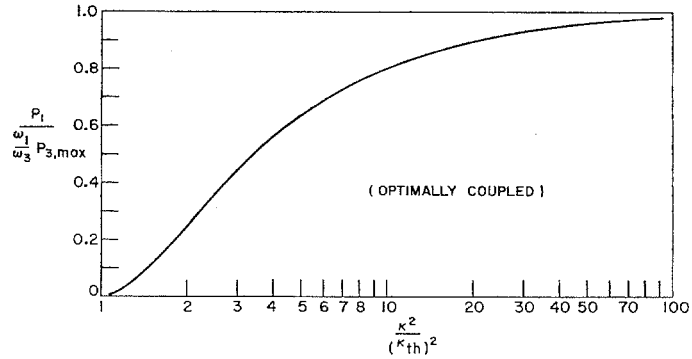

Fig. 5. Optimally coupled signal output power.

conditions, focusing, or crystal nonlinearity. Therefore, the ratio of κ to κ_{th} is a realistic variable and represents the strength of the nonlinear interaction with respect to the strength required for threshold.

Figs. 2 to 4 display some characteristics of the oscillator for the efficient steady-state operation of (27a) to (27c). These figures show the form of the onset of oscillation and the buildup of power for the signal for typical laser operating parameters. In each case the dotted lines indicate the onset of the pulsing output of the oscillator and are continued to show where the steady-state solution would have operated.

In Fig. 2, E_1^2 and E_3^2 are plotted versus laser gain. For the parameters chosen in this case, the laser reaches its oscillation threshold at a gain of 3 percent per pass and increases in power until the parametric oscillator reaches threshold. At that point, the laser limits and further increases in gain result in signal (and idler) power.

In Figs. 3 and 4 the pump and signal power are plotted versus κ^2/κ_{th}^2; $E_{3,max}^2$ is the value that the square of pump electric field amplitude has in the absence of parametric oscillation. As the parametric interaction increases, the pump power continually decreases. Simultaneously, the signal power first increases, goes through a maximum, and begins to decrease. Qualitatively, this can be understood as the result of the fact that the parametric interaction appears to be an increasing loss to the laser. Eventually, the total available power from the gain mechanism goes through a maximum and begins to decrease, much in the same way that increasing output coupling losses to a laser can produce a similar maximum in output power.

In order to determine the efficiency of the oscillator, one must determine the proper output coupling to the signal for given operating conditions. In terms of the ratio κ^2/κ_{th}^2, the efficiency of the oscillator is independent of all other parameters.

The optimum coupling to the signal is found by maximizing the output signal power P_1 with respect to α_{1c}. In a manner analogous to (25), P_1 is given by

$$P_1 = \gamma \alpha_{1c} E_1^2. \tag{37}$$

In terms of the maximum available pump power $P_{3,max}$, the maximization produces, when optimally coupled, the result

$$P_1 = \frac{\omega_1}{\omega_3} P_{3,max} \left[1 - \left(\frac{\kappa_{th}}{\kappa} \right)^2 \right]^2. \tag{38}$$

With perfect conversion, the Manley–Rowe relations limit the signal power to be ω_1/ω_3 times the pump power. Therefore, we see that the internal oscillator satisfies this condition since that is the asymptotic value that the signal power approaches. Fig. 5 is a plot of the relation given by (38). From this graph it is apparent that once the oscillator is above threshold it rapidly becomes very efficient.

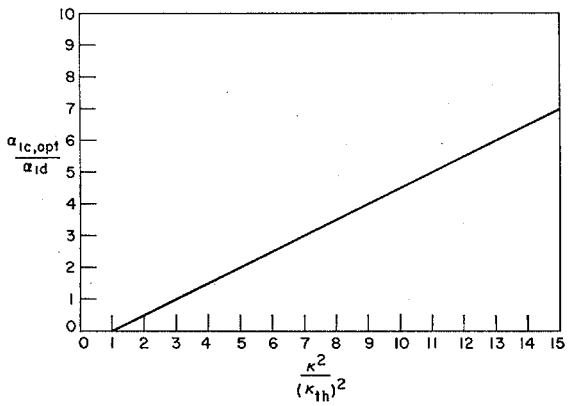

Fig. 6. Ratio of optimum signal coupling loss to signal dissipative loss.

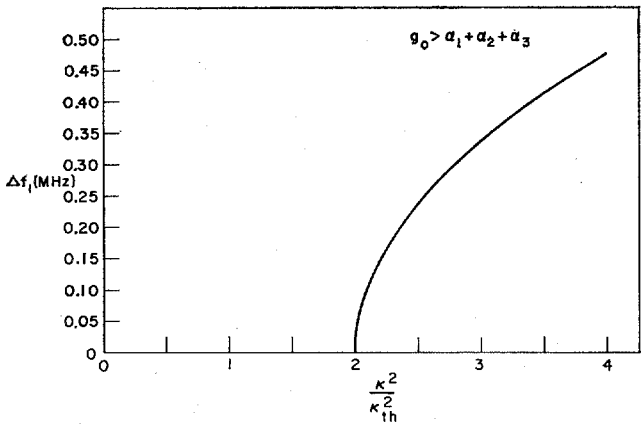

Fig. 7. Frequency shift of signal versus $(\kappa/\kappa_{th})^2$.

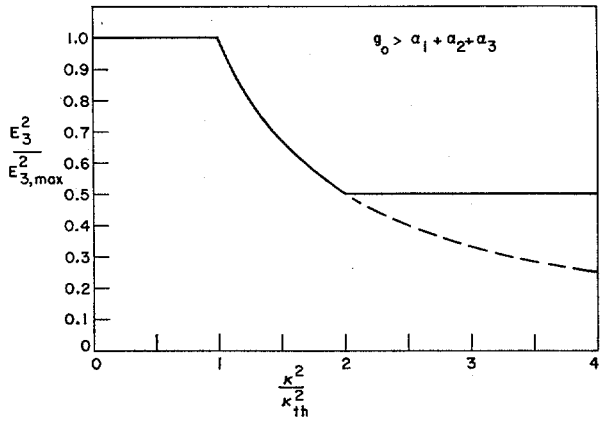

Fig. 8. Pump power versus $(\kappa/\kappa_{th})^2$ showing onset of inefficient region of operation.

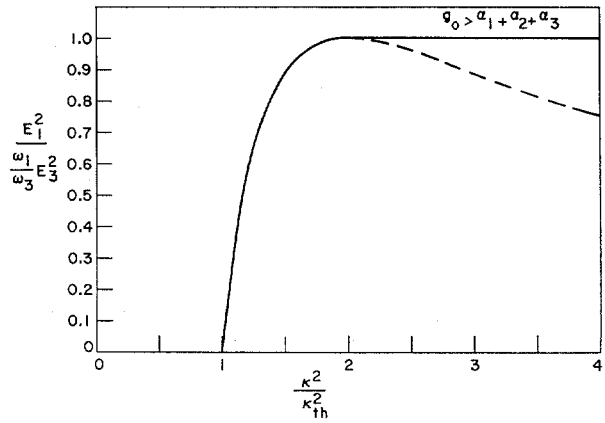

Fig. 9. Signal power versus $(\kappa/\kappa_{th})^2$ showing onset of inefficient region of operation.

Fig. 6 is a plot of the optimum ratio of coupling loss to dissipative loss versus κ^2/κ^2_{th} and is given by

$$\frac{\alpha_{1c,opt}}{\alpha_{1d}} = \frac{1}{2}\left[\left(\frac{\kappa^2}{\kappa^2_{th}}\right) - 1\right]. \tag{39}$$

Combining these results with the stability condition given by (32), it is possible to show that should efficient operation be desired, no pulsing output will be experienced so long as optimum coupling to the signal is maintained.

D. Inefficient Steady-State Region of Operation

The steady-state region of operation described by (28a) to (28d) represents a case in which the parametric interaction drives the phases of the signal, idler, and pump rather than their amplitudes, thereby resulting in less efficient operation. In general, this is probably a region to be avoided in almost any practical case by appropriately adjusting the operating parameters of the oscillator. Nevertheless, its characteristics are important in understanding the behavior of the internal oscillator.

In (20d) of Section II only one equation was written for all the phases. This equation is the sum of three equations of the form

$$\frac{d\phi_1}{d\tau} = \frac{\omega_1 L}{C}\chi_1' + \frac{\omega_1 \kappa E_2 E_3}{E_1}\cos(\phi_3 - \phi_1 - \phi_2). \tag{40}$$

The fact that $\phi_1 + \phi_2 - \phi_3 =$ a constant results from the relations that

$$\dot{\phi}_1 = \Delta\omega_1 \tag{41a}$$

$$\dot{\phi}_2 = \Delta\omega_2 \tag{41b}$$

$$\dot{\phi}_3 = \Delta\omega_3, \tag{41c}$$

where $\Delta\omega_1 + \Delta\omega_2 - \Delta\omega_3 = 0$. That is, $\dot{\phi}_i$ is a constant, representing a shift in frequency of ω_i to $\omega_i + \Delta\omega_i$. These frequency shifts are given by the following equations:

$$\Delta\omega_1 = \alpha_1 \cot(\phi_3 - \phi_1 - \phi_2) \times \frac{c}{2L} \tag{42a}$$

$$\Delta\omega_2 = \alpha_2 \cot(\phi_3 - \phi_1 - \phi_2) \times \frac{c}{2L} \tag{42b}$$

$$\Delta\omega_3 = (\alpha_1 + \alpha_2) \cot(\phi_3 - \phi_1 - \phi_2) \times \frac{c}{2L}, \tag{42c}$$

where

$$\sin^2(\phi_3 - \phi_1 - \phi_2) = \frac{g_0\beta\alpha_1\alpha_2}{g_0 - \alpha_1 - \alpha_2 - \alpha_3}\frac{1}{\omega_1\omega_2\kappa^2}. \tag{43}$$

The shifts are on the order of a megahertz as shown by Fig. 7 for typical operating parameters.

Figs. 8 and 9 show the behavior of the internal oscillator,

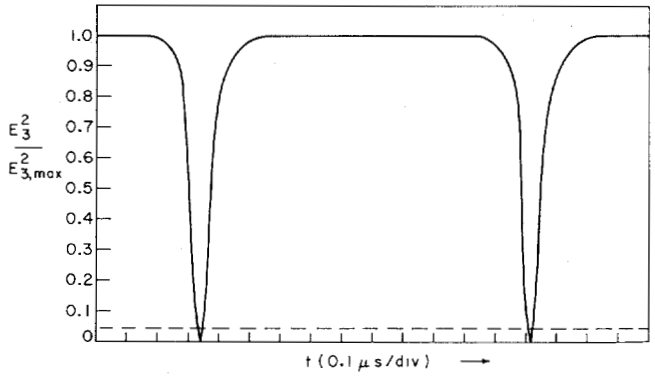

Fig. 10. Pump power versus time in pulsing region of operation.

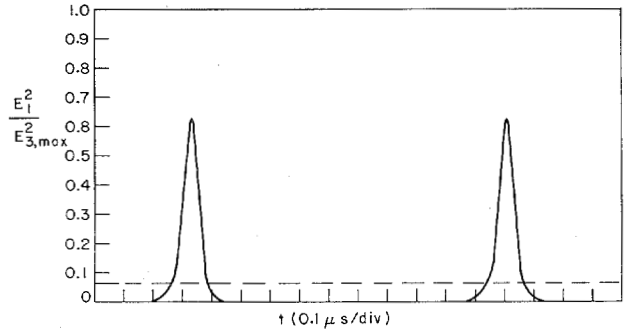

Fig. 11. Signal power versus time in pulsing region of operation.

which is able to operate in this inefficient region. The dotted curves represent the behavior had the oscillator remained in the other steady-state region. Once the value of κ^2 is large enough to reach threshold for this second type of steady-state operation, then the pump and signal power no longer change for increasing parametric interaction. The fact that the signal power limits at a maximum in Fig. 9 is a coincidence of the particular parameters chosen for plotting the curve.

It is difficult to decide exactly what is the physical reason for this type of operation. However, we can make some comments that do aid in understanding this behavior.

First we notice that the expression for the pump power (proportional to E_3^2) has very much the same form as the similar expression for pump power in the case of no parametric oscillation. The only difference is that α_3 is replaced by $\alpha_1 + \alpha_2 + \alpha_3$. In addition, a threshold condition for this region of operation is $g_0 > \alpha_1 + \alpha_2 + \alpha_3$, which is similar to the threshold condition for the laser with, once more, the laser loss replaced by the sum of the losses to signal, idler, and pump. For these reasons, one is led to speculate that in this region of operation, the laser appears to have its gain mechanism coupled directly to all three circuits: signal, idler, and pump. Then all three frequencies oscillate with many characteristics similar to a laser rather than a laser pumped parametric oscillator.

Since there are two solutions possible under the condition that $g_0 > \alpha_1 + \alpha_2 + \alpha_3$, the question then arises as to why the system picks one mode of operation as opposed to the other. By investigating the second threshold condition, i.e.,

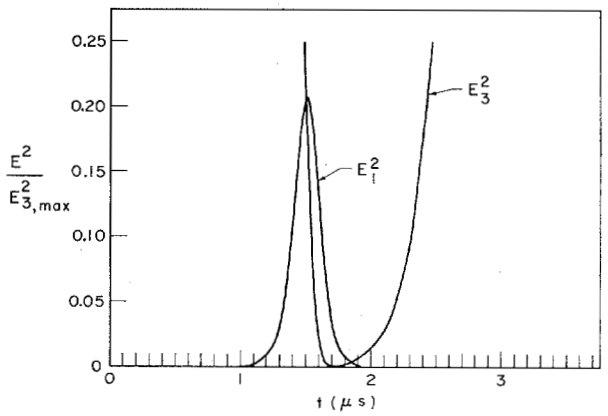

Fig. 12. Details of one pump and signal pulse.

$$\kappa^2 \geq \frac{\alpha_1\alpha_2}{\omega_1\omega_2}\,\frac{g_0\beta}{g_0 - \alpha_1 - \alpha_2 - \alpha_3}$$

one then finds a result similar to the maximum-emission principle proposed by Statz, DeMars, and Tang [47]. The systems pick the mode of operation which maximizes the pump power.

E. Pulsing Output of Internal Parametric Oscillator

The purpose of this section is to describe the characteristics of the internal oscillator in its pulsing mode of operation. It has been impossible to find the solutions for this region of operation in closed form. Therefore, a computer analysis of (20a) to (20d) was used to solve for the behavior in this region. The objective has been to outline the qualitative behavior of this spiking regime, and laser parameters were chosen that we believe are representative of existing lasers and materials.

Before proceeding, it is pointed out that we have not used any rate equation approach [48] in developing the equations of motion. Therefore, for some very slow atomic mechanisms (e.g., for use with CO_2 lasers) another equation must be included to account for population changes of the energy levels. Nevertheless, for most lasers, the results of this analysis appear to be consistent with the assumption that no rate equation is necessary.

Figs. 10 and 11 show typical results for the signal and pump fields as a function of time in the pulsing region of operation. The dotted lines represent the corresponding levels had pulsing not begun. The computer analysis has been carried out through many pulses and these appear to be constant in peak height and period. We therefore characterize this region of operation as a repetitively pulsing regime.

Fig. 12 shows an expanded version of one pulse, pointing out the relation between the signal and pump during the course of one pulse. Using this graph we can qualitatively explain the physical reason for this type of operation.

Since the oscillator is well above threshold (because of the stability condition of (32)), the signal and idler build up very rapidly. (As is well known, the buildup time of a parametric oscillator decreases as the margin above

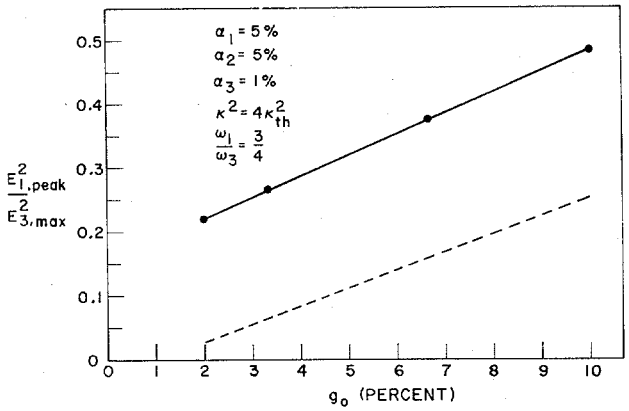

Fig. 13. Peak signal power versus laser gain.

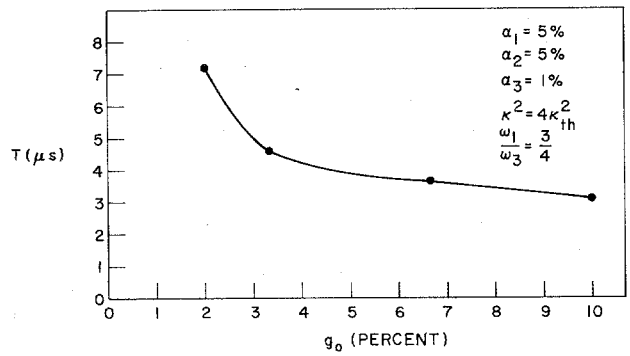

Fig. 14. Pulse period versus laser gain.

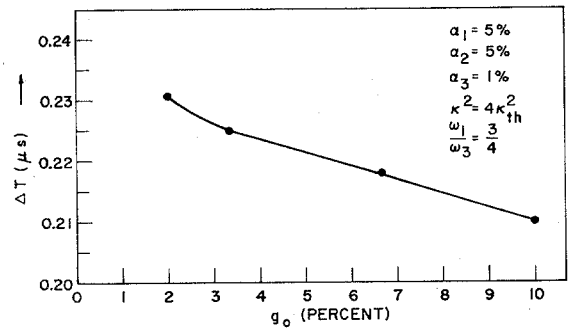

Fig. 15. Pulse width versus laser gain.

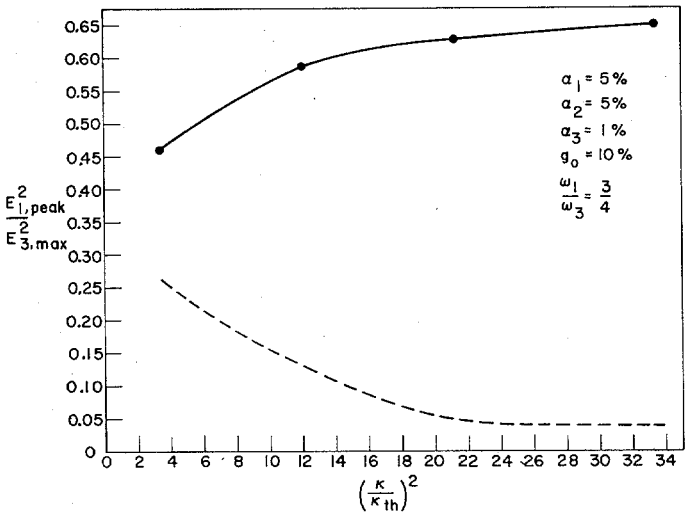

Fig. 16. Peak signal power versus $(\kappa/\kappa_{th})^2$.

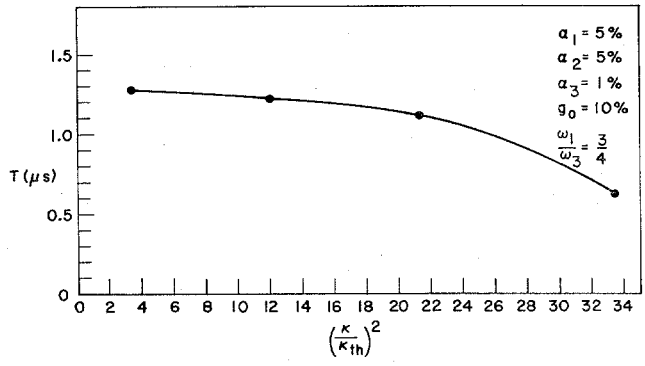

Fig. 17. Pulse period versus $(\kappa/\kappa_{th})^2$.

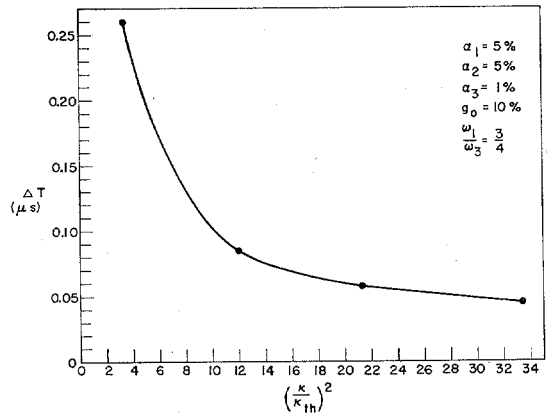

Fig. 18. Pulse width versus $(\kappa/\kappa_{th})^2$.

threshold increases.) The pump is slowed in its decay somewhat by the bandwidth of its resonance. Therefore the signal and idler buildup past the point to which they should have approached, thus draining more power from the pump. As a result, the pump experiences sufficient effective loss to go below threshold. The continuing decrease of the pump is eventually felt by the signal and idler and they then decrease rapidly. With no signal and idler present the pump can once more buildup to its free running value and the process repeats.

Figs. 13 to 15 display the change in pulse parameters as the gain of the laser is changed. The dotted line in Fig. 13 is proportional to the signal power in the steady-state region of operation. Here T is the period between pulses and ΔT is the full width of the pulses between one-half power points. As the gain of the laser is increased, the peak power in the pulses increases and their period and width decrease.

In Figs. 16 to 18 the same characteristics of the pulses are plotted versus κ^2/κ^2_{th}. As κ^2 increases, again the peak power of the pulses increases, and their period and width decrease.

IV. Efficiency of an External Parametric Oscillator

In this section we briefly describe the results of a calculation of the efficiency of an external parametric oscillator having pump, signal, and idler resonated [49]. Once the oscillator is above threshold, reflections of the pump from the active cavity can lead to reduced efficiency from the oscillator. Therefore, a central concern of the calculation is that these reflections be taken into account.

The details of the calculation are not included here, although the technique is summarized. Beginning with the normal mode formulation of Slater [50], the input fields at the pump appear as surface integrals on the cavity boundaries. Reflections are accounted for by energy losses of the internal fields at the mirrors. The calculation leads to second order partial differential equations for the amplitudes of the normal modes at the signal, idler, and pump frequencies. The procedure is very similar to the technique used by Gordon and Rigden [51] in analyzing the Fabry–Perot electrooptic modulator, and the partial differential equations for the mode amplitudes of the parametric oscillator are a straightforward extension of their work.

The result of the calculation of signal power P_1 yields

$$\frac{P_1}{P_3} = \frac{\omega_1}{\omega_3}\frac{\alpha_{3c}}{\alpha_3}\left[\frac{\alpha_{1c}}{\sqrt{(\alpha_{1c}+\alpha_{1d})\alpha_{1d}}}\frac{\kappa_{th}}{\kappa} - \frac{\alpha_{1c}}{\alpha_{1d}}\left(\frac{\kappa_{th}}{\kappa}\right)\right]^2, \tag{44}$$

where P_3 is the incident pump power and α_{3c} is the transmission loss necessary for coupling pump power into the resonator. Therefore, α_3 consists of two parts, coupling loss α_{3c} and dissipative loss α_{3d}. In this expression, κ/κ_{th} is reduced from its previously defined value by the ratio α_{3c}/α_3.

Defining

$$\beta = \frac{\alpha_{1c}}{\alpha_{1d}} \tag{45}$$

the expression for P_1/P_3 can be written as

$$\frac{P_1}{P_3} = \frac{\omega_1}{\omega_3}\frac{\alpha_{3c}}{\alpha_3} f(\beta), \tag{46}$$

where

$$f(\beta) = \frac{\kappa_{th}}{\kappa}\frac{\beta}{\sqrt{1+\beta}} - \frac{\beta\kappa_{th}^2}{\kappa^2}. \tag{47}$$

Maximizing $f(\beta)$ yields the coupling to the signal that produces maximum output power. Fig. 19 is a plot of this function maximized with optimum coupling $f(\beta_m)$. On the same scale we have plotted the efficiency of the internal parametric oscillator $(\omega_3 P_1/\omega_1 P_{3,max})$ also in terms of $(\kappa/\kappa_{th})^2$ for that oscillator.

There could be some objection to displaying the data in this form. However, with a brief explanation it becomes useful in comparing the relative efficiencies of the two oscillators. To the extent that the crystal represents no dissipative loss to the pump (in the form of absorption, scattering, or reflection), the value of κ/κ_{th} is the same in both the internal and external cases. Any real crystal will present some loss, however.

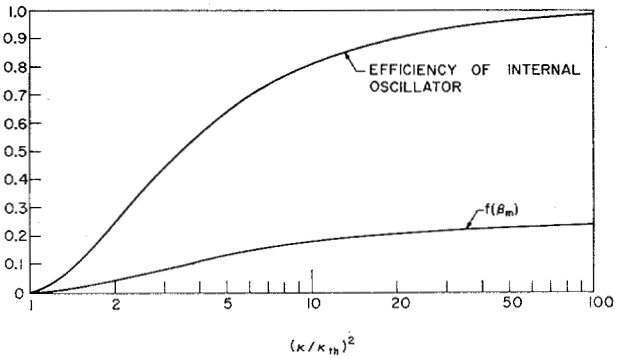

Fig. 19. Efficiency of external parametric oscillator.

The effect on the internal oscillator will be to lower the pump power through its dependence on losses. The extent of this reduction depends basically on the gain of the laser medium and the relative magnitude of the crystal losses with respect to other dissipative losses. Typically, the insertion of a crystal inside a laser cavity may reduce the laser power by 25 to 50 percent [52] with a comparable reduction in $(\kappa/\kappa_{th})^2$.

The effect of crystal losses at the pump wavelength is readily apparent in the case of the external oscillator. First $(\kappa/\kappa_{th})^2$ is reduced by the factor $(\alpha_{3c}/\alpha_{3c}+\alpha_{3d})^2$ and at a given value of κ/κ_{th}, the output power is reduced by the factor $\alpha_{3c}/\alpha_{3c}+\alpha_{3d}$. It seems reasonable to assume that in many cases the net effect of losses will therefore result in comparable percentage reductions of power in the internal and external cases. Based on this reasoning we can therefore use Fig. 19 to compare the output power of the internal and external oscillators in the case of no losses at the pump and conclude that this is similar to their relative efficiency in the case with losses. However, we caution that this is only a rule of thumb, which could be slightly different for very high-gain or very low-gain lasers.

We can draw some fairly firm conclusions on the relative merits of the internal and external oscillators from these curves. The efficiency of the external oscillator is greatly reduced due to reflections of the pump from the active cavity. As a result, in cases where the crystal losses inserted into the laser do not substantially reduce the laser power (for example to the point that the laser itself is only slightly above threshold), the internal oscillator should produce the higher output power. In addition, the difficulty of coupling the pump into the external oscillator will make the internal oscillator more useful in practice.

V. Summary and Conclusions

Having solved the equations of motion for a parametric oscillator internal to the laser cavity and thereby coupled directly to the saturating gain mechanism of the laser, we have found that such an oscillator can operate in three distinctly different regimes: an efficient regime, a re-

petitively pulsing regime, and an inefficient regime characterized by frequency shifts of the pump, signal, and idler. The necessary conditions for operation in one particular mode have been derived in terms of the stability criteria for that regime. The regimes are mutually exclusive and may be chosen by varying the laser gain, the oscillator output coupling, or the crystal nonlinearity.

To some extent, each regime may be useful in practice. The pulsing regime offers peak powers slightly greater than the average power of the CW regimes, although the average power is somewhat lower. Some control of repetition rate and length of the pulses is available through changes in the laser gain and crystal nonlinearity. The inefficient regime is generally less useful than the other two regimes, although some applications might make use of the several megahertz frequency shifts of the pump, signal, and idler.

The efficient regime is probably of greatest interest. An important result of the analysis shows that this regime is capable of approaching 100 percent efficiency in conversion of pump power to signal and idler power. By way of comparison, the efficiency of an external oscillator, with pump, signal, and idler resonated, is limited to about 25 percent.

Acknowledgment

It is a pleasure to acknowledge many helpful discussions with B. Byer, A. E. Siegman, E. O. Ammann, and W. B. Tiffany. Mrs. Cora Barry expertly prepared the computer programs.

References

[1] N. M. Kroll, "Parametric amplification in spatially extended media and applications to the design of tuneable oscillators at optical frequencies," *Phys. Rev.*, vol. 127, pp. 1207–1211, August 15, 1962.
[2] J. K. Wright, "Enhancement of second harmonic power generated by a dielectric crystal inside a laser cavity," *Proc. IEEE*, vol. 51, p. 1663, November 1963.
[3] R. G. Smith, K. Nassau, and M. F. Galvin, "Efficient continuous optical second-harmonic generation," *Appl. Phys. Letters*, vol. 7, pp. 256–258, November 15, 1965.
[4] A general treatment of parametric amplifier and oscillator techniques with an extensive bibliography is given by W. H. Louisell, *Coupled Mode and Parametric Electronics*. New York: Wiley, 1960.
[5] R. H. Kingston, "Parametric amplification and oscillation at optical frequencies," *Proc. IRE*, vol. 50, p. 472, April 1962.
[6] S. A. Akhmanov and R. V. Khokhlov, *Zh. Eksperim i Theor. Fiz.*, vol. 43, pp. 351–353, July 1962 (transl.: "Concerning one possibility of amplification of light waves," *Soviet Phys.—JETP*, vol. 16, pp. 252–254, January 1963).
[7] J. A. Armstrong, N. Bloembergen, J. Ducuing, and P. S. Pershan, "Interactions between light waves in a nonlinear dielectric," *Phys. Rev.*, vol. 127, pp. 1918–1939, September 15, 1962.
[8] G. D. Boyd and A. Askin, "Theory of parametric oscillator threshold with single-mode optical masers and observation of amplification in $LiNbO_3$," *Phys. Rev.*, vol. 146, pp. 187–198, June 3, 1966.
[9] V. N. Lugovoy, *Radiotekhn. i Electron.*, vol. 9, p. 596, 1964 (transl.: "A cavity parametric amplifier and oscillator," *Radio Eng. Electron.*, vol. 9, pp. 483–492, April 1964).
[10] S. A. Akhmanov, V. G. Dmitriyev, V. P. Modenov, and V. V. Fadeev, *Radiotekhn. i Electron.*, vol. 10, p. 2157, 1965 (transl.: "Parametric generation in a resonator filled with a nonlinear dielectric," *Radio Eng. Electron.*, vol. 10, pp. 1841–1849, December 1965).
[11] S. A. Akhmanov and R. V. Khokhlov, *Usp. Fiz. Nauk.*, vol. 88, pp. 439–484, March 1966 (transl.: "Parametric amplifiers and generators of light," *Soviet Phys.—Usp.*, vol. 9, pp. 210–222, September–October 1966).
[12] A. Yariv and W. H. Louisell, "Theory of the optical parametric oscillator," *IEEE J. Quantum Electronics*, vol. QE-2, pp. 418–424, September 1966.
[13] J. A. Giordmaine, "Mixing of light beams in crystals," *Phys. Rev. Letters*, vol. 8, pp. 19–20, January 1, 1962.
[14] P. D. Maker, R. W. Terhune, M. Nisenoff, and C. M. Savage, "Effects of dispersion and focusing on the production of optical harmonics," *Phys. Rev. Letters*, vol. 8, pp. 21–22, January 1, 1962.
[15] S. A. Akhmanov, A. I. Kovrigin, R. V. Khokhlov, and O. N. Chunaev, *Zh. Eksper. i Theor. Fiz.*, vol. 45, pp. 1336–1343, November 1963 (transl.: "Coherent interaction length of light waves in a nonlinear dielectric," *Soviet Phys.—JETP*, vol. 18, pp. 919–924, April 1964).
[16] J. E. Midwinter and J. Warner, "The effects of phase matching method and of uniaxial crystal symmetry of the polar distribution of second-order non-linear optical polarization," *Brit. J. Appl. Phys.*, vol. 16, pp. 1135–1142, August 1965.
[17] D. A. Kleinman, "Theory of second harmonic generation of light," *Phys. Rev.*, vol. 128, pp. 1761–1775, November 15, 1962.
[18] J. E. Bjorkholm, "Optical second-harmonic generation using a focused gaussian laser beam," *Phys. Rev.*, vol. 142, pp. 126–136, February 1966.
[19] D. A. Kleinman, A. Ashkin, and G. D. Boyd, "Second-harmonic generation of light by focused laser beams," *Phys. Rev.*, vol. 145, pp. 338–379, May 6, 1966.
[20] N. Bloembergen and P. S. Pershan, "Light waves at the boundary of non-linear media," *Phys. Rev.*, vol. 128, pp. 606–622, October 15, 1962.
[21] G. D. Boyd, A. Ashkin, J. M. Dziedzic, and D. A. Kleinman, "Second-harmonic generation of light with double refraction," *Phys. Rev.*, vol. 137, pp. A1305–A1320, February 15, 1965.
[22] A. Ashkin, G. D. Boyd, and J. M. Dziedzic, "Resonant optical second-harmonic generation and mixing," *IEEE J. Quantum Electronics*, vol. QE-2, pp. 109–124, June 1966.
[23] S. A. Akhmanov, V. G. Dmitriev, and V. P. Modenov, *Radiotekhn. i Electron.*, vol. 10, p. 649, 1965 (transl.: "On the theory of frequency multiplication in a cavity resonator filled with a nonlinear medium," *Radio Eng. Electron.*, vol. 10, pp. 552–559, April 1965).
[24] C. C. Wang and C. W. Racette, "Measurement of parametric gain accompanying optical difference frequency generation," *Appl. Phys. Letters*, vol. 6, pp. 169–171, April 15, 1965.
[25] S. A. Akhmanov, A. I. Kovrigin, A. S. Piskarskas, V. V. Fadeev, and R. V. Khokhlov, *Zh. Eksperim. i Theor. Fiz., Pis'ma Redakt.*, vol. 2, pp. 300–305, 1965 (transl.: "Observation of parametric amplification in the optical range," *JETP Letters*, vol. 2, pp. 191–193, October 1, 1965).
[26] S. A. Akhmanov, A. G. Ershov, V. V. Fadeev, R. V. Khokhlov, O. N. Chunaev, and E. M. Shvom, *Zh. Eksperim. i Theor. Fiz., Pis'ma Redakt.*, vol. 2, pp. 458–463, 1965 (transl.: "Observation of two-dimensional parametric interaction of light waves," *JETP Letters*, vol. 2, pp. 285–288, November 15, 1965).
[27] J. E. Midwinter and J. Warner, "Up-conversion of near infrared to visible radiation in lithium-meta-niobate," *J. Appl. Phys.*, vol. 38, pp. 519–523, February 1967.
[28] J. A. Giordmaine and R. C. Miller, "Tunable coherent parametric oscillation in $LiNbO_3$ at optical frequencies," *Phys. Rev. Letters*, vol. 14, pp. 973–976, June 14, 1965.
[29] S. A. Akhmanov, A. I. Kovrigin, V. A. Kolosov, A. S. Piskarskas, V. V. Fadeev, and R. V. Khokhlov, *Zh. Eksperim. i Theor. Fiz., Pis'ma Redakt.*, vol. 3, pp. 372–378, 1966 (transl.: "Tunable parametric light generator with KDP crystal," *JETP Letters*, vol. 3, pp. 241–245, May 1, 1966).
[30] R. C. Miller and W. A. Nordland, "Tunable $LiNbO_3$ optical oscillator with external mirrors," *Appl. Phys. Letters*, vol. 10, pp. 53–55, January 15, 1967.
[31] L. B. Kreuzer, "Ruby-laser-pumped optical parametric oscillator with electro-optic effect tuning," *Appl. Phys. Letters*, vol. 10, pp. 336–338, June 15, 1967.
[32] R. G. Smith, J. E. Geusic, H. J. Levinstein, J. J. Rubin, S. Singh, and L. G. Van Uitert, "Continuous optical parametric oscillation in $Ba_2NaNb_5O_{15}$," *Appl. Phys. Letters*, vol. 12, pp. 308–310, May 1, 1968.
[33] I. T. Ho and A. E. Siegman, "Passive phase-distortionless parametric limiting with varactor diodes," *IRE Trans. Microwave Theory and Techniques*, vol. MTT-9, pp. 459–472, November 1961.
[34] S. E. Harris and O. P. McDuff, "Theory of FM laser oscillation," *IEEE J. Quantum Electronics*, vol. QE-1, pp. 245–262, September 1965.
[35] W. E. Lamb, Jr., "Theory of an optical maser," *Phys. Rev.*, vol. 134, pp. A1429–A1450, June 15, 1964.
[36] G. D. Boyd, R. C. Miller, K. Nassau, W. L. Bond, and A. Sav-

age, "$LiNbO_3$: An efficient phase matchable nonlinear optical material," *Appl. Phys. Letters*, vol. 5, pp. 234–236, December 1, 1964.
[37] R. C. Miller, G. D. Boyd, and A. Savage, "Nonlinear optical interactions in $LiNbO_3$ without double refraction," *Appl. Phys. Letters*, vol. 6, pp. 77–79, February 15, 1965.
[38] P. S. Pershan, "Non-Linear Optics," in *Progress in Optics V*, E. Wolf, Ed. New York: Wiley, 1966.
[39] D. A. Kleinman, "Nonlinear dielectric polarization in optical media," *Phys. Rev.*, vol. 126, pp. 1977–1979, June 15, 1962.
[40] R. H. Kingston and A. L. McWhorter, "Electromagnetic mode mixing in nonlinear media," *Proc. IEEE*, vol. 53, pp. 4–12, January 1965.
[41] J. Warner, D. S. Robertson, and K. F. Hulme, "The temperature dependence of optical birefringence in lithium niobate," *Phys. Letters*, vol. 20, pp. 163–164, February 1, 1966.
[42] R. C. Miller and A. Savage, "Temperature dependence of the optical properties of ferroelectric $LiNbO_3$ and $LiTaO_3$," *Appl. Phys. Letters*, vol. 9, pp. 169–171, August 15, 1966.
[43] W. W. Rigrod, "Gain saturation and output power of optical masers," *J. Appl. Phys.*, vol. 34, pp. 2602–2609, September 1963.
[44] A. E. Siegman, "Obtaining the equations of motion for parametrically coupled oscillators or waves," *Proc. IEEE*, vol. 54, pp. 756–762, May 1966.
[45] J. La Salle and S. Lefschetz, *Stability by Liapunov's Direct Method*. New York: Academic Press, 1961.
[46] D. F. Tuttle, Jr., *Network Synthesis*. New York: Wiley, 1958.
[47] H. Statz, G. A. DeMars, and C. L. Tang, "Self-locking of modes in lasers," *J. Appl. Phys.*, vol. 38, pp. 2212–2222, April 1967.
[48] A. Yariv, *Quantum Electronics*. New York: Wiley, 1967.
[49] M. K. Oshman, "Studies of optical frequency parametric oscillation," Stanford University, Stanford, Calif., M. L. Rept. 1602, 1967.
[50] J. C. Slater, *Microwave Electronics*. New York: Van Nostrand, 1950.
[51] E. I. Gordon and J. D. Rigden, "The Fabry–Perot electrooptic modulator," *Bell Sys. Tech. J.*, vol. 42, pp. 155–179, January 1963.
[52] R. Targ, L. M. Osterink, and J. M. French, "Frequency stabilization of the FM laser," *Proc. IEEE*, vol. 55, pp. 1185–1192, July 1967.

Correspondence

Current Noise Spectra of GaAs Laser Diodes in the Luminescence Mode

***Abstract*—The current noise of GaAs laser diodes in the luminescence mode has been measured at frequencies between 0.47 kHz and 1.5 MHz. A $1/f$ behavior is found at relatively lower frequencies. In the investigated frequency range, the noise level is considerably higher than $2 \cdot e \cdot I \cdot \Delta f$.**

In a recent paper, Haug [1] calculated the current noise spectrum of a semiconductor laser junction for frequencies small compared to the reciprocal radiative lifetime but high enough for the flicker noise to be unimportant. Current noise measurements [2] in luminescent junctions are reported for frequencies up to about 10 kHz. This correspondence reports some results of our investigations on current noise of GaAs laser diodes in the luminescence mode at an ambient temperature of 293°K. The diodes were forward biased, and the measurements were made in the frequency range between 0.47 kHz and 1.5 MHz.

The noise measuring setup consisted of a high-input impedance preamplifier followed by the main amplifier, filters, and a true rms voltmeter. In the lower frequency range, active filters [3] have been used in contrast with the high-frequency range where a heterodyne voltmeter has been employed. The diode dc current was supplied by a filtered battery.

Several diffused GaAs diodes have been tested. The donor concentrations ranged from 4×10^{17} cm^{-3} to 3×10^{18} cm^{-3}. When driven with pulses at 77°K, the diodes had a lasing threshold current between 0.85 A and 2.4 A. The junction areas ranged from 0.3×10^{-3} cm^2 to 1×10^{-3} cm^2. The measured mean-square noise current $\overline{i_n^2}$ at an effective bandwidth of 1 Hz as a function of frequency is shown in Figs. 1 and 3 for four dc forward biased laser diodes The current noise spectrum of the diodes $D9$ and $D13$ (Fig. 1) is approximately $1/f$ noise. In the vicinity of about 0.7 MHz, the mean-square noise current tends to become constant. This results in a time constant of about $\tau_m = 2.3 \times 10^{-7}$ seconds, see [4], [5]. It is tempting to compare the measured amount of noise with some noise level associated with the diode current I. It has been pointed out [2] that $\overline{i_n^2}$ for a GaAs luminescent diode is many orders of magnitude larger than the shot noise given by the formula $2e \cdot I \cdot \Delta f$. This statement is confirmed by our investigations. However, the comparison of the measured amount of noise with $2e \cdot I \cdot \Delta f$ may lead to confusion. Indeed, the shot noise in p-n junctions, where the current is carried by diffusion, is given by $2e \cdot (I + 2I_s) \cdot \Delta f$, I_s representing the saturation current [6]. This formula holds as long as the frequency f, associated with Δf, is small compared to the reciprocal lifetime of the minority carriers and the reciprocal of their transit time through the depletion layer. Now, in forward biased GaAs p-n junctions, the current is mainly composed of the following three components: 1) diffusion current, proportional to $\exp(eV/kT)$; 2) recombination current in the space-charge region, proportional to $\exp(eV/2kT)$; and 3) tunneling current, proportional to $\exp(\alpha \cdot V)$, where α is independent of the temperature. Surface recombination may also cause a contribution. For the current densities of interest, the current–voltage characteristics of our diodes showed the tunneling component of the current to be negligible. The current was proportional to $\exp(eV/mkT)$ with m ranging between 1 and 2

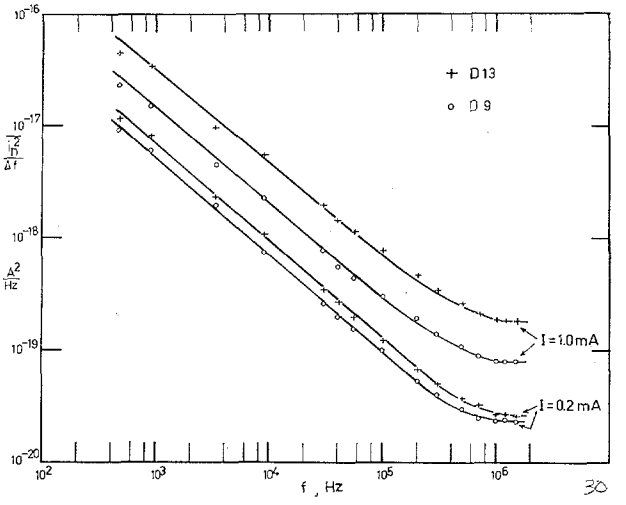

Fig. 1. Mean-square noise currents $\overline{i_n^2}$ at an effective bandwidth of 1 Hz as a function of frequency f for the diodes $D9$ and $D13$.

Manuscript received January 25, 1968.